Appl. Magn. Reson. (2008) 35, 15–32
DOI 10.1007/s00723-008-0140-6
Printed in The Netherlands

Applied
Magnetic Resonance

Phase Cycling in Electron Spin Echo Envelope Modulation

S. Stoll and **B. Kasumaj**

Physical Chemistry Laboratory, Swiss Federal Institute of Technology Zurich,
Zurich, Switzerland

Received 22 October 2007

Abstract. We present a general way to devise efficient phase cycles for arbitrary electron spin echo envelope modulation (ESEEM) experiments. The method determines all coherence transfer pathways contributing to the measured signal, selects those of interest and then examines all possible nested phase cycles in order to find those that achieve the required selection. The procedure is used to find efficient nested phase cycles for ESEEM sequences containing up to nine pulses: two-pulse, three-pulse and five-pulse ESEEM, standard and six-pulse hyperfine sublevel correlation (HYSCORE) as well as their extensions including remote echo detection. In addition, it is shown that by shifting the last pulse by 90°, three-pulse ESEEM and HYSCORE do not need phase cycling in the case of a symmetrically excited line.

1 Introduction

In nuclear magnetic resonance (NMR) and pulse electron paramagnetic resonance (EPR), multiple-pulse sequences produce a series of free induction decays (FIDs) and echoes. Among these, only one is of actual interest. All the others distort the measurement, but can be removed by phase cycling [1–3], a procedure where the pulse sequence is repeated several times with different pulse phases and the resulting signals are linearly combined so that all signal contributions except the wanted echo or FID cancel. Even though the general principles of phase cycling have been laid out in 1984 [1], it continues to attract interest in NMR [4–12]. In EPR, the only work entirely dedicated to phase cycling was published in 1990 [2], although phase cycles for specific experiments appear in various places, e.g., refs. 13–17.

This work was initiated by attempts to devise appropriate phase cycles for five-pulse electron spin echo envelope modulation (ESEEM) [14] and six-pulse hyperfine sublevel correlation (HYSCORE) [15] as well as their combinations with remote echo detection [16], yielding pulse sequences with eight and nine pulses, respectively [17]. These sequences are too long to allow for a straightforward intuitive design based on the principles outlined in ref. 2, and a more systematic

approach was desirable, which we now summarize in this work. Using this approach, we examined several often employed ESEEM sequences with and without remote echo detection and computed phase cycles for all of them. Although some of them are not new, it might be beneficial to have all of them compiled in one place. As an unexpected twist resulting from our systematic investigations, we discovered phase-shifted variants of three-pulse ESEEM and HYSCORE where crossing echoes are out of phase with respect to the echo of interest and thus do not need phase cycling in the case of a symmetrically excited line.

In this paper we proceed as follows. First, facts about coherence transfer pathways in ESEEM are summarized, as they form the basis of the theory behind phase cycling. The effect of pulse phases on measured signals is discussed and the concept of phase cycling is introduced. This is followed by a description of the method used to devise phase cycles, consisting of a selection of relevant pathways, proper phasing of the pulses, and a systematic search for appropriate phase cycles. We then derive old and new phase cycles for a series of ESEEM experiments. Numerical simulations and experimental demonstrations are included.

2 Background

As shown in Fig. 1a, a general ESEEM pulse sequence consists of a series of N microwave pulses P_i separated by $N-1$ periods (delays) of free evolution of length t_i. The ESEEM signal, the amplitude of an electron spin echo from the paramagnetic sample, is detected after a delay of length t_N after the last pulse. The delay lengths can be written in vector form

$$\mathbf{t} = (t_1,\ t_2,\ ...,\ t_N).$$

In the following, let us assume that the lengths of the pulses and the width of the detection window are negligible with respect to the delay lengths t_i. This

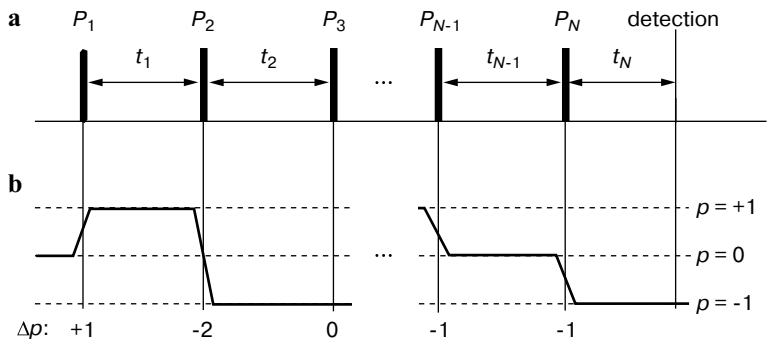

Fig. 1. a General ESEEM pulse sequence consisting of N microwave pulses P_i followed by N intervals of free evolution (delays) of length t_i. **b** Example of a coherence transfer pathway for a spin system consisting of one electron spin. p is the coherence order, Δp the change in p induced by a pulse.

assumption does not invalidate the final results, but alleviates the notational burden considerably.

In an ESEEM experiment, the echo amplitude is measured as a function of one or several delay lengths, giving one-, two-, or, in general, D-dimensional time-domain data. Along each dimension d, some of the delays are prolonged or shortened in K_d steps ($k_d = 0, ..., K_d - 1$), independently (e.g., in HYSCORE) or simultaneously (e.g., in the 2-D sum combination frequency experiment [18]). At step k_d, the increment of a delay is $k_d\ dt_{i,d}$, where $dt_{i,d}$ is the step length of delay i along dimension d. The vector of all delays at a given acquisition point $\mathbf{k} = (k_1, ..., k_D)$ is

$$\mathbf{t}(\mathbf{k}) = \mathbf{t}_0 + d\mathbf{t} \cdot \mathbf{k}. \tag{1}$$

$\mathbf{t}_0 = (t_{1,0}, ..., t_{N,0})$ is the vector of initial delay lengths $t_{i,0}$, and $d\mathbf{t}$ is an $N \times D$ matrix with $dt_{i,d}$ as elements, completely specifying the incrementation scheme of the ESEEM experiment. Often, there are only one or two dimensions and at most two incremented delays per dimension. For example, for a HYSCORE experiment with a step length of $dt_{2,1} = dt_{3,2} = \Delta$ in both dimensions, the vector of delay lengths of Eq. (1) is

$$\mathbf{t} = \begin{pmatrix} \tau \\ T_0 \\ T_0 \\ \tau \end{pmatrix} + \begin{pmatrix} 0 & 0 \\ \Delta & 0 \\ 0 & \Delta \\ 0 & 0 \end{pmatrix} \cdot \begin{pmatrix} k_1 \\ k_2 \end{pmatrix} = \begin{pmatrix} \tau \\ T_0 + k_1\Delta \\ T_0 + k_2\Delta \\ \tau \end{pmatrix}.$$

Phase cycling is based on the concept of coherence order [1, 2]. For a diluted sample of paramagnetic centers containing one electron with spin $S = 1/2$ each, there are three possible (electron) coherence orders. Coherence order 0 corresponds to longitudinal magnetization and is due to spins parallel or antiparallel to the external magnetic field direction. Coherence orders $+1$ and -1 (henceforth abbreviated as $+$ and $-$) represent transverse magnetization and correspond to spins rotating in a plane perpendicular to the external field. Coherences with order 0, $+$ and $-$ correspond to the S_z, S_+ and S_- components of the density operator, respectively [19].

As microwave pulses nutate only electron spins, it is sufficient for our purpose to consider electron coherence orders only. If nuclei are coupled to the electron spin, nuclear coherences of various orders are possible, which modulate the amplitude of the echo signal. The presence of these modulations, however, is not relevant to the design of the phase program. For the purpose of simulating ESEEM signals [20–22], it is useful to distinguish between zero-order electron coherence in the α and β manifolds (spin-up and spin-down, designated as 0_α and 0_β, corresponding to the S_α and S_β components in the density operator) [17]. For phase cycling, however, this distinction is superfluous.

Before the first pulse, the electron spins are in thermal equilibrium, and only polarization corresponding to coherence order zero exists ($p_0 = 0$). A pulse P_i

transfers magnetization from any order $p_i - 1$ to one or several or all of the possible orders p_i. During free evolution, the coherence order does not change. Thus, during the pulse sequence, the magnetization divides into several independent portions that undergo different sequences of coherence order changes. They travel along different coherence transfer pathways [1], characterized by the history of coherence orders p_i during the N free evolution periods

$$\mathbf{p} = (p_1,\ p_2,\ ...,\ p_N)$$

or, alternatively, by the sequence of coherence order changes $\Delta p_i = p_i - p_{i-1}$ induced by the N pulses,

$$\Delta\mathbf{p} = (\Delta p_1,\ \Delta p_2,\ ...,\ \Delta p_N),$$

where the coherence order before the first pulse is $p_0 = 0$ for all pathways, as already mentioned. Δp_i can have values from -2 to $+2$. An example of an electron coherence transfer pathway is shown in Fig. 1b. Since there are three coherence orders, the number of possible pathways increases by a factor of three with each pulse, and there are a total of 3^N pathways after N pulses. For two-pulse ESEEM, there are 9 possible pathways: (+, +), (+, 0), (+, −), (0, +), (0, 0), (0, −), (−, +), (−, 0), and (−, −). The fraction of spins following each of the pathways will of course depend on the flip angles of the pulses.

In an EPR sample, the resonance frequencies ω_S of the spins are distributed, and only very few spins are resonant with the spectrometer frequency ω_{mw}. Most spins have a resonance frequency offset $\Omega_S = \omega_S - \omega_{\mathrm{mw}} \neq 0$ and acquire a phase $\exp(-\mathrm{i}p\Omega_S t)$ during free evolution, where p is the coherence order. Whenever all spins with different Ω_S are in phase, a signal in the form of an FID or an echo is observable.

Each pathway gives rise to an FID and possibly a number of echoes. The FID occurs after a pulse that converted coherence from the initial order 0 to ± 1. The echoes occur at times when the spins have spent equal amounts of time in coherence of order $+1$ and -1, which can happen several times along a pathway. We will denote the last of these refocusing points in time, measured relative to the detection point, as the in-phase time Δt of the pathway. It depends, in addition to the sequence of coherence orders of a given pathway, on all delay lengths and is given by

$$\Delta t(\mathbf{t}) = \sum_i p_i t_i = \mathbf{p}\cdot\mathbf{t}. \tag{2}$$

If $\Delta t = 0$, the FID or echo maximum occurs exactly at the detection point, whereas a negative (positive) Δt means that it occurs before (after) the detection. For example, the echo due to (0, +, −) in three-pulse ESEEM with delays denoted (τ, T, τ) occurs at $\Delta t = 0\cdot\tau + (+1)\cdot T + (-1)\cdot\tau = T - \tau$ relative to the detection point.

Note that we assign exactly one echo or FID to each pathway. E.g., the pathway (+, +) describes the FID after the first pulse, and (+, −) describes the echo

after the second pulse. Actually, all the + coherence after the first pulse contributes to the FID, and part of it is then refocused and forms the echo. Here, we divide this coherence into two parts, where the coherence assigned to (+, +) is the one contributing to the FID only, and the coherence assigned to (+, −) is the one then forming the echo. Formally, therefore, (+, +) corresponds to the FID, and (+, −) corresponds the echo alone. This is viable, since we are only interested in the phase behavior, and not on the actual coherence transfer amplitudes.

Together with a D-dimensional incrementation scheme for the t_i (Eq. (1)), the dependence of Δt in Eq. (2) on $\mathbf{k}$ is

$$\Delta t(\mathbf{k}) = \Delta t_0 + \Delta \mathbf{t}_1 \cdot \mathbf{k},$$

where $\Delta t_0 = \mathbf{p} \cdot \mathbf{t}_0$ and $\Delta \mathbf{t}_1 = \mathbf{p} \cdot d\mathbf{t}$. As the acquisition proceeds, echoes and FIDs change their position with respect to the detection point, and Δt changes, sometimes changing sign. For each pathway, Δt varies between a minimum and a maximum value

$$\Delta t_{\min} = \Delta t_0 + (\mathbf{K} - 1) \cdot \min(\Delta \mathbf{t}_1, 0), \tag{3}$$

$$\Delta t_{\max} = \Delta t_0 + (\mathbf{K} - 1) \cdot \max(\Delta \mathbf{t}_1, 0), \tag{4}$$

with $\mathbf{K} = (K_1, \ldots, K_D)$.

Each pulse has a phase ϕ_i relative to the receiver reference phase [23]. Experimentally, only four pulse phases are used in ESEEM: 0° (x), 90° (y), 180° ($-x$, abbreviated by $\bar{x}$), and 270° ($-y, \bar{y}$). Others are technically more difficult to implement and calibrate. A quadrature detector acquires signals in two channels, channel A with phase 0° (x) and channel B with 90° (y). Quadrature detection measures signals from pathways with $p_N = -1$, all other pathways are invisible. In the case of two-pulse ESEEM, the pathways visible to a quadrature detector are (+, −), (0, −) and (−, −). Although quadrature detection is rarely used in ESEEM, we use it in the pathway analysis, as it is necessary for understanding the phase separation of signals.

After digitization of the two signals S_A and S_B, they are combined into one complex signal $S = S_A + iS_B$ in the computer. In a phase program, signals of experiments with different pulse phasings (called the steps in the phase program) are linearly combined to yield a total signal where undesired signal contributions are eliminated. The linear combination (LC) coefficients are of the form $\exp(i\phi_{dig})$, where ϕ_{dig} is the post-digitization phase [23]. With the four pulse phases given above, there are only four LC coefficients needed to create all possible distinct signal combinations: $+1$, $+i$, -1 and $-i$.

The linear combination of the signals from the different steps can be performed directly during the acquisition as part of signal averaging, or alternatively during data processing on the computer, as it is done in the spectrometer we use for our experiments.

For designing phase programs, the phase behavior of pathway signals upon changes of pulse phases is essential. A signal of a pathway with coherence pass-

ing through an order change of Δp_i under the action of pulse i reacts to a change $\Delta\phi_i$ of the pulse phase by changing its phase ψ by $\Delta\psi_i = -\Delta p_i \Delta\phi_i$ [1][1]. More generally, if several pulse phases are changed simultaneously, the total signal phase shift is

$$\Delta\psi = -\sum_i \Delta p_i \Delta\phi_i = -\Delta\mathbf{p}\cdot\Delta\boldsymbol{\phi}\,. \tag{5}$$

As a result of the pulse phase shifts, the pathway signal acquires an additional phase factor of $\exp(\mathrm{i}\Delta\psi) = \exp(-\mathrm{i}\Delta\mathbf{p}\Delta\boldsymbol{\phi})$. The phase-shifting property Eq. (5) is the basis for removing or avoiding disturbing signals in ESEEM experiments.

3 Pathway List

In order to devise an effcient phase program for an ESEEM experiment, all pathways that significantly contribute to or disturb the measured signal have to be determined. This is done in several steps.

(1) At the outset, all possible detectable pathways starting with $p_0 = 0$ and ending in $p_N = -1$ are enumerated. This depends only on the number N of pulses, not on the incrementation scheme. Each pulse increases the number of pathways by a factor of 3, so there are a total of 3^{N-1} detectable pathways. E.g., for a three-pulse sequence ($N = 3$) there are 9 pathways: (−, −, −), (−, 0, −), (0, −, −), (0, 0, −), (−, +, −), (0, +, −), (+, +, −), (+, 0, −), and (+, −, −).

(2a) Next, if the transverse relaxation time T_{2e} of the electron spins is known, all pathways along which coherence completely relaxes before the detection can be excluded. A pathway signal is decaying due to transverse relaxation during all delays where it has coherence order $|p| = 1$. A pathway does not lead to a significant signal if $|\mathbf{p}|\cdot\mathbf{t}(\mathbf{k}) \gg T_{2e}$ for all $\mathbf{k}$. (In the common case that all increments $dt_{i,d}$ are positive, this means $|\mathbf{p}|\cdot\mathbf{t}_0 \gg T_{2e}$.) This relaxational removal of pathways is sometimes used experimentally in remote echo detection [16], where the time T_{re} between the 90° storage pulse and the first pulse of the two-pulse reading sequence is usually set to $T_{re} > 5T_{2e}$ so that coherences with $p = \pm 1$ during this period relax. The spins relaxing during a delay i leave their current pathway and enter the all-zero order pathway $p_1 = \ldots = p_i = 0$, so that they can contribute again to other pathways, e.g., the FID after pulse P_{i+1}.

(2b) The amplitude of the coherence transfer effected by a pulse depends on its flip angle. By computing the total transfer amplitudes for each pathway, one could determine which coherence transfer pathways give rise to significant

---

[1] The sign in this expression has to be carefully considered. For spins with $\gamma < 0$ like the electron, it is negative, as stated. For $\gamma > 0$, the most common case in NMR, it would be positive. However, the negative sign can be used if $\Delta\phi_i$ is redefined as $-\mathrm{sign}\gamma$ times the electronic phase shift. For more details about these sign issues, see refs. 3 and 6.

echoes and which do not. In the limit of infinitely short pulses, a 180° pulse only transfers + to −, − to + and 0 to 0. For real-world pulses more than a few nanoseconds long and spectra broader than the excitation bandwidth of these pulses, such a picture is too simplistic, and transfer amplitudes are diffcult to quantify. In addition, a pulse can have different flip angles for different EPR transitions, especially in high-spin systems. For these reasons, we will not take transfer amplitudes into account. Our phase cycles work for arbitrary pulse flip angles.

(3) Next, we exclude another set of pathways from the further analysis: Any pathway with an in-phase point that never comes close to the detection point is invisible during the entire experiment (over the full domain of **k**) and can be neglected. An invisible pathway satisfies

$$\Delta t_{\max} < -\Delta t_{\lim} \text{ or } \Delta t_{\min} > \Delta t_{\lim}, \tag{6}$$

where the value of $\Delta t_{\min}$ is determined by the width of the detection window and the widths of echoes and FIDs. In practice, it is suffcient to set $\Delta t_{\lim}$ to a value of twice the full width at half maximum (FWHM) of the echo, for example, 50 ns. Any pathway whose in-phase point comes closer than this value to the detection point contributes to the detected signal. Echo pathway visibility can only be determined by going through Eqs. (3), (4) and (6). On the other hand, the case of FID pathways is simpler: The FID after the last pulse, from (0, ..., 0, −), is invisible if $t_{N,0} > \Delta t_{\lim}$ (provided that the last delay is not decremented). In that case, that is, if the FID after the last pulse does not overlap with the measured portion of the echo, all other FIDs are invisible, too.

After the three-stage selection process, the remaining visible pathways fall into two different categories. Signals from pathways with

$$\Delta t_{\min} > -\Delta t_{\lim} \text{ and } \Delta t_{\max} < \Delta t_{\lim}$$

lie in the detection window for all points **k**, they are focused. Some of them have $\Delta t_{\min} = \Delta t_{\max} = 0$ and consequently $\Delta t = 0$ for all **k**. All other visible pathways give signals that cross the detection window at some points **k** during the acquisition, they are crossing.

Each visible pathway can be either wanted or unwanted. The contributions from crossing pathways are unwanted, as they lead to spikes and similar transients in the time-domain signal. A properly designed phase program should give a total signal free of contributions from these pathways. Most of the times, the signal from all the focused pathways are wanted and should add up. For simple pulse sequences, there is often only one focused pathway. For some sequences, some focused pathways are unwanted, e.g., the primary echo from the last two pulses in five-pulse ESEEM, (0, 0, 0, +, −). If there is more than one wanted pathway, the relative phase between the signals from these pathways is relevant, and the phase program must be designed in an appropriate way. We will examine this next.

4 Initial Pulse Phases

Before we can continue to examine phase programs, the initial phases of the pulses have to be chosen. If all pulses have identical phase – which is the case for most common ESEEM experiments –, all FIDs and echoes occur out of phase with respect to the pulses. The in-phase part of the signal vanishes for symmetric inhomogeneously broadened lines excited at the center. If the pulses have x phase, all signals have $\pm y$ phase. This can be visualized by considering the resonant spins only, i.e., those with $\Omega_S = 0$. Any pulse with x or $-x$ phase rotates them in the yz plane of the rotating frame, and as they do not acquire an additional phase during free evolution, they never leave that plane.

The relative phases between pulses are relevant when there are several wanted pathways, as their signals can interfere constructively or destructively, depending on the pulse phases. A proper phase choice depends on what interferences are possible and on what is to be measured. A prominent example of this is the five-pulse ESEEM experiment, where a relative phase of $\pm 90°$ between the first and the third pulse ensures that the signals from the two pathways of interest, (+, −, 0, +, −) and (−, +, 0, +, −), have opposite phases and subtract, so that the nuclear modulation can be observed. This is discussed in detail in Sect. 6.

In addition to determining the interference between wanted pathways, the relative phases between pulses can be used to phase-separate wanted and unwanted signals: by phase shifting the last pulse in a sequence by $\pm 90°$, all pathways that are not affected by the last pulse ($\Delta p_N = 0$) do not change their phase, whereas all other signals are phase-shifted by $\pm 90°$ or $\pm 180°$ (see Eq. (5)). In ESEEM experiments, all $\Delta p_N = 0$ signals are unwanted, therefore an at least partial phase separation of wanted and unwanted signals can be achieved by such a last-pulse shift. Surprisingly, this works in three-pulse ESEEM and HYSCORE and reduces the number of steps necessary in phase cycling. In Sect. 6, we examine this in detail.

5 Phase Cycling

With a full list of wanted and unwanted pathways and properly phased pulses to achieve the desired relative phase between wanted pathways, we can proceed to determining suitable phase programs that remove unwanted pathways. Although attempts have been made to compute them directly from the list of wanted and unwanted pathways [5], it can in general only be done by examining a list of possible phase programs. Here we restrict ourselves to the original and most common class of phase programs, nested phase cycles. More recent and unconventional schemes like cogwheel phase cycles [6, 10] or noncycling phase programs [5] have been shown to yield programs with fewer steps in some cases in NMR, though their utility in EPR, with its much smaller numbers of pulses and coherence orders, still remains to be evaluated.

In a nested phase cycle, the phases of pulses or pulse blocks are cycled independently, in a nested fashion. For example, when in a three-pulse sequence

with starting phases *xyx* the first and second pulse are blocked together and cycled through 180° and the third pulse is cycled through 90° independently of the first two, the following sequence of phase cycle steps is obtained: *xyx*, *xyy*, $xy\bar{x}$, $xy\bar{y}$, $\bar{x}y\bar{x}$, $\bar{x}y\bar{y}$, $\bar{x}\bar{y}\bar{x}$ and $\bar{x}\bar{y}\bar{y}$. By convention, the rightmost block is cycled first, i.e., it forms the innermost of the nested loops. We use a shorthand notation for such nested phase cycles. The sequence of pulse phases of the first step in the phase cycle is written, and pulses or blocks of pulses are enclosed in parentheses if they are cycled. Parentheses (...) indicate cycles in 180° steps, and square brackets [...] indicate 90° cycles. The example above would be written (*xy*)[*x*]. This notation does not include the LC coefficients, which have to be listed separately in order to fully specify the phase cycle.

The search for effective phase cycles proceeds as follows. In a first stage, all possible nested phase cycles for the given number of pulses are listed. To achieve this, all possible pulse blockings are generated. For example, the possible blockings in a three-pulse sequence are 111, 112, 122, 123, where each number indicates which block a pulse is assigned to. Each of the blocks in a blocking can now be cycled in 360° (no cycling), 180° or 90° steps, thus yielding a number of phase cycles for each blocking. In our example, the blocking 112 gives the two-step cycles 11(2) and (11)2, the four-step cycles 11[2], (11)(2) and [11]2, as well as the eight-step cycles [11](2) and (11)[2] and the 16-step cycle [11][2].

In the second stage, the LC coeffcients necessary to select the wanted pathways are computed for all steps in each cycle. For this, one of the wanted pathways *c*, with coherence order change vector $\Delta\mathbf{p}^{(c)}$, is chosen as a pivot, and its signal phase $\psi^{(c)}$ for each individual step is computed $\psi^{(c)} = \psi_0^{(c)} - \boldsymbol{\phi} \cdot \Delta\mathbf{p}^{(c)}$, where $\boldsymbol{\phi}$ is the vector of pulse phases (shifts from zero phase). The LC coefficient necessary for this step in the phase cycle is thus $\exp(\mathrm{i}\psi^{(c)})$, since the pulse-phase independent $\exp(\mathrm{i}\psi_0^{(c)})$ can be factored out and neglected.

With all the LC coeffcients determined, the list of nested phase cycles can be shortened, as it contains many cycles that are equivalent to others. This becomes clear from the following. If the phases of all pulses are changed simultaneously by the same amount $\Delta\phi$, then according to Eq. (5) the signal phase changes by $\Delta\psi = -\Delta\phi(p_N^{(c)} - p_0)$. For the observable pathways with $p_0 = 0$ and $p_N^{(c)} = -1$, this means that $\Delta\psi = \Delta\phi$. Thus, rotating all pulse phases and the LC coefficient in a step by the same amount leaves all pathway signals of that step unaffected. Therefore, every phase program is part of a class of equivalent phase programs, where the individual steps differ only in their absolute phase and their LC coefficients. In each class, all phase programs but one can be dropped. We always keep one that removes the receiver DC offset, i.e., one where the sum over all steps of the LC coefficient is zero. An example of two equivalent phase cycles is (*xx*)*x* with LC coefficients $+1$, $+1$ and *xx*(*x*) with $+1$, -1. The latter one eliminates any receiver offset and is therefore preferable.

Each of the phase cycles can now be examined in turn for its effectiveness. For this, the signal phases of all pathways are computed for each step of the phase cycle and then linearly combined using the LC coefficients. If the result is zero, the pathway is eliminated by the phase cycle, otherwise, it is retained.

Phase cycles are often chosen to have the smallest possible number of steps. In principle, the number of steps has no impact on the signal-to-noise ratio per time, but as many spectrometers have an overhead reprogramming time between steps of a phase cycle, the number of steps matters in practice. If two phase cycles have the same number of steps, those with the smallest number of pulse phases needed are usually preferred, since they are easier to set up experimentally. The specific design of the spectrometer (number of available pulse phases, channels with fixed phases versus channels with fast phase switching) might also influence the choice.

6 ESEEM Experiments

In the following we use the methodology outlined above to examine phase cycles for several standard ESEEM experiments. This is accompanied by numerical simulations and experimental verifications. All phase cycles discussed below are summarized in Table 1, including the LC coeffcients, which we omit in the text for readability.

All experimental data (three-pulse ESEEM and HYSCORE) were acquired at room temperature on a Bruker ElexSys E580 spectrometer at around 9.7 GHz. Accurate measurement parameters are given in the legends of the figures where the data are shown. For all experiments, Pittsburgh coal was used as a sample.

6.1 Two-Pulse ESEEM

The two-pulse ESEEM experiment, [90°–τ–180°–τ–detect] is very simple: The only pathway of interest is (+, −), and (0, −) and (−, −) are the only (potentially) disturbing ones. The phase cycle $(x)x$ removes both a receiver DC offset and (0, −), i.e., unwanted signals due to the last pulse (FID, and ring-down after pulse). The pathway (−, −) does not normally interfere. If it does, a four-step cycle $x[x]$ can be used.

6.2 Three-Pulse ESEEM

The three-pulse ESEEM experiment, [90°–τ–90°–T–90°–τ–detect], is traditionally set up with all three pulses having the same phase, xxx. The amplitude of the stimulated echo from (+, 0, −) is measured as a function of T, and a four-step phase cycle $x(x)(x)$ is normally used to remove the signals due to crossing echoes [19]. The echoes from (0, +, −) and (−, +, −) cross at $T = \tau$ and $T = 2\tau$, thus have to be suppressed. This can be achieved by the simple two-step cycle $xx(x)$. The echoes from (+, +, −) and (+, −, −) cross at $T = 0$, but as the signal is acquired only for $T \geq T_0 > 0$, they rarely disturb.

If the FID from the last pulse (0, 0, −) does not decay before the stimulated echo, it is eliminated by the four-step cycle $x(x)(x)$, which is therefore preferable

Table 1. Phase cycles for ESEEM experiments.

Experiment[a]	Pulse phases[b]	LC coefficients[b]	Notes[c]
2p ESEEM	$(x)x$	+1, −1	leaves (−, −)
	$x[x]$	+1, −1, +1, −1	complete
3p ESEEM	$xx(x)$	+1, −1	leaves (−, 0, −), FID
	$x(x)(x)$	+1, −1, −1, +1	leaves (−, 0, −)
	$x[x](x)$	+1, −1, −i, +i, −1, +1, +i, −i	complete
HYSCORE	$xx(x)(x)$	+1, −1, +1, −1	leaves (−, 0, 0, −), FID
	$x(x)(x)(x)$	+1, −1, +1, −1, −1, +1, −1, +1	leaves (−, 0, 0, −)
	$x[x](x)(x)$	+1, −1, +1, −1, −i, +i, −i, +i, −1, +1, −1, +1, +i, −i, +i, −i,	complete
5p ESEEM	$yyx(xx)$	+1, −1	leaves FID; 2p ooph
	$yy(x)(xx)$	+1, −1, −1, +1	sp
	$y[y](x)xx$	+1, −1, −1, +1, +1, −1, −1, +1	complete for $\Delta t_{\mathrm{lim}} = 0$
6p HYSCORE	$yyx(x)(xx)$	+1, −1, +1, −1	leaves FID; 2p ooph
	$yy(x)(x)(xx)$	+1, −1 +1, −1, −1, +1, −1, +1	sp
2p ESEEM re	$x[x]xxx$	+1, −1, +1, −1	leaves (±, ∓, 0, 0, −)
	$x(x)x(x)x$	+1, −1, +1, −1	leaves 2p; (+, +, 0, −, −)
	$x[x]x(x)x$	+1, +1, −1, −1, +1, +1, −1, −1	complete for $\tau_{\mathrm{re}} > \tau$
3p ESEEM re	$xx(xxxx)$	+1, −1	leaves FID, 2p
	$(x)(x)xxxx$	+1, −1, −1, +1	
	$(x)(x)xxx(x)$	+1, +1, −1, −1, −1, −1, +1, +1	for $\tau_{\mathrm{re}} = 2\tau$
HYSCORE re	$xx(x)(xxxx)$	+1, −1, +1, −1	leaves FID, 2p
	$(x)(x)(x)xxxx$	+1, +1, −1, −1, −1, −1, +1, +1	
5p ESEEM re	$yyx(xxyyy)$	+1, −1	keeps all focused, FID
	$(yy)(x)xxyyy$	+1, −1, −1, +1	(±, ∓, 0, 0, 0, 0, +, −) ooph
	$(yy)(x)(x)xyyy$	+1, −1, −1, +1, +1, −1, −1, +1	
6p HYSCORE re	$yyx(x)(xxyyy)$	+1, −1, +1, −1	keeps all focused, FID
	$(yy)(x)(x)xxyyy$	+1, +1, −1, −1, −1, −1, +1, +1	(±, ∓, 0, 0, 0, 0, 0, +, −) ooph
	$(yy)(x)(x)(x)xyyy$	+1, −1, +1, −1, −1, +1, −1, +1, −1, +1, −1, +1, +1, −1, +1, −1	

[a] p, pulse; re, remote echo detection.
[b] Notation explained in text.
[c] FID: FID after last pulse; 2p: two-pulse echo generated by the last two pulses; ooph: out of phase; sp: for $\tau_1 \neq \tau_2$, $\tau_1 \neq 2\tau_2$, $2\tau_1 \neq \tau_2$ only.

to the two-step cycle. It turns out that it does not remove the delayed FID from (−, 0, −). In the rare case where this contribution is significant, an eight-step cycle $x[x](x)$ has to be used.

Surprisingly, phase cycling can be avoided if the nonstandard pulse phases *xxy* are used. By shifting the third pulse phase by ±90° relative to the first two, the phases of all crossing echoes are shifted by 180°, whereas the stimulated echo is shifted by ±90°. That is, the echo of interest and the disturbing ones appear in different receiver channels. If the spectral hole generated by the first pulse is symmetric, signals from the crossing echoes are completely absent from the receiver channel that contains the three-pulse echo, and phase cycling is not necessary.

In ESEEM, echoes give only one nonzero signal, the orthogonal-phase signal being zero, unless the spectral hole burned by the first pulse is not symmetric

around the carrier frequency. This can happen, if the EPR line shape varies significantly over the excitation width of the pulse or if the excitation profile of the pulse itself is not symmetric, e.g., if the spectrometer frequency does not exactly match the frequency of the resonance mode. In these cases, a residual signal is visible with phase orthogonal to the echo. The integral of this signal over a small interval centered on the echo, however, can still be very small, as the positive and negative regions of the signal cancel.

The interesting phase separation of the echoes is experimentally demonstrated in Fig. 2. Five echoes from (+, −, −), (+, 0, −), (−, +, −), (0, +, −) and (+, +, −) are visible. They all appear in one channel when the pulse phases *xxx* are used (Fig. 2a). For the pulse phases *xxy*, all echoes after the last pulse change sign, and the stimulated echo from (+, 0, −) moves to the other channel, which is, apart from small out-of-phase residues, free of the other echoes. As is seen in Fig. 2b, the modulated decay of the stimulated echo is similarly free of echo crossing artifacts. The FID from (0, 0, −) is shifted by 90°, just as the stimulated echo, and a two-step cycle (*x*)*xy* should be used if it disturbs.

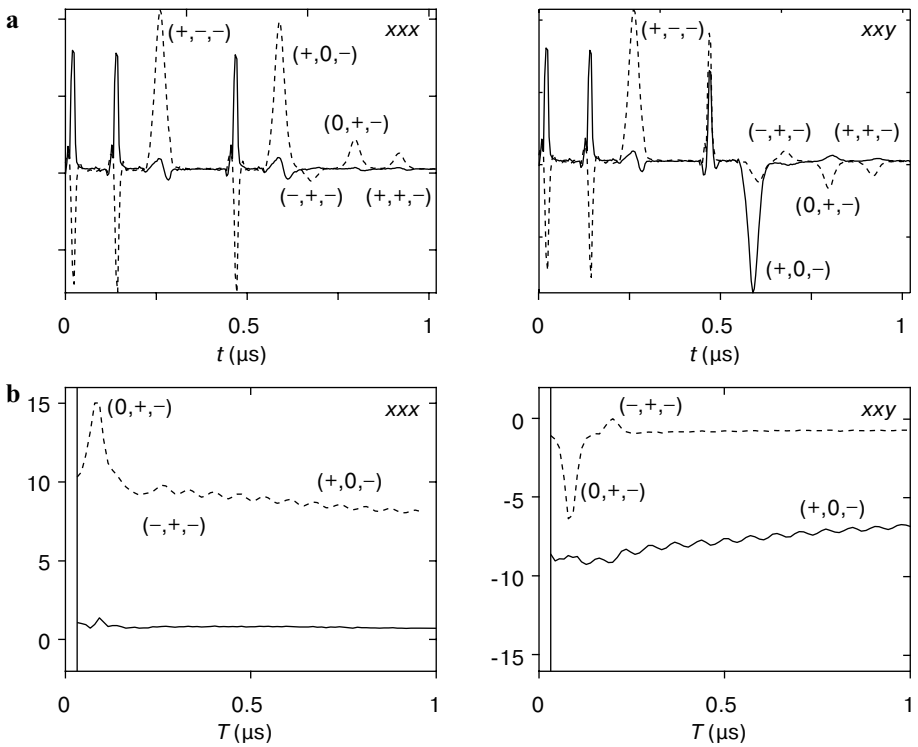

Fig. 2. Three-pulse ESEEM measurements on Pittsburgh coal (9.695 GHz, 345.49 mT, room temperature). Pulse lengths 16 ns, pulse phases *xxx* (left) and *xxy* (right). **a** Transients (τ = 140 ns, T = 420 ns). **b** Echo amplitude modulations (τ = 100 ns, T_0 = 48 ns). Solid lines, receiver channel A (phase 0°); dashed lines, receiver channel B (phase 90°).

6.3 HYSCORE

In the HYSCORE experiment, [90°–τ–90°–t_1–180°–t_2–90°–τ–detect], the signal is acquired as a two-dimensional function of t_1 and t_2. Similar to the three-pulse ESEEM experiment, the HYSCORE experiment is carried out with all four pulses having identical phases, *xxxx*. A total of 18 disturbing echoes can appear with the same phase as the HYSCORE echo from (+, 0, 0, −), as illustrated by a simulation in Fig. 3a. These echoes give rise to spurious signals, since they cross the detection point along several lines in the (t_1,t_2) domain. In Fig. 3b, these crossing echo lines and the corresponding pathways are shown schematically.

To remove the disturbing signals, Gemperle et al. [2] have devised several phase cycles, depending on whether the pulses can be considered ideal and whether FIDs are negligible. The case of ideal pulses is of little practical relevance. For nonideal pulses, the four-step cycle *xx*(*x*)(*x*) removes all crossing echoes and is the most commonly used. It retains the pathways (−, 0, 0, −) and (0, 0, 0, −). If the signal from the latter (FID or the ringing of the last pulse) overlap with the echo, an eight-step cycle *x*(*x*)(*x*)(*x*) should be used. In the highly unlikely case that the signal from (−, 0, 0, −), a delayed FID, interferes, the 16-step program *x*[*x*](*x*)(*x*) can eliminate it.

If the last pulse is shifted by ±90°, a phase separation between the HYSCORE echo and the majority of unwanted crossing echoes can be achieved, similar to three-pulse ESEEM. This is shown in Fig. 3a. The unwanted crossing echoes remaining in phase with the HYSCORE echo are from the pathways (+, −, 0, −), (+, +, 0, −), (0, +, 0, −) and (−, +, 0, −) and cross the HYSCORE echo at $t_1 = 0,\ \tau,\ 2\tau$, independent of t_2, as illustrated in Fig. 3b. Because these crossings appear parallel to the t_2 axis in the acquired data, they can be easily removed by

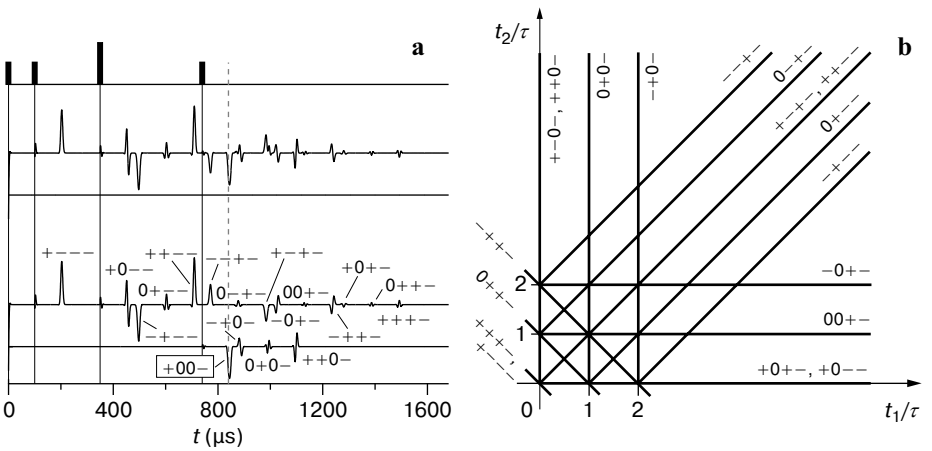

Fig. 3. a Phases of echoes in the HYSCORE sequence. Upper two traces: phasing *xxxx*, lower two traces: phasing *xxxy*. Note that the signal from (+, −, 0, −) cannot be observed for the shown delay lengths (τ = 100 ns, t_1 = 250 ns, t_2 = 390 ns). **b** Position of all 14 unwanted echo crossings in the HYSCORE time-domain signal, generated by 18 disturbing echoes, labelled by their associated pathways.

a linear baseline correction along t_2. Therefore, phase cycling can be avoided if the phasing *xxxy* or $xxx\bar{y}$ is used.

Figure 4 gives an experimental demonstration of this scheme. In Fig. 4a, the signal resulting from the sequence with the standard phases *xxxx* is shown. All echoes appear in the lower channel, the residuals in the upper channel are very weak. For the pulse phasing $xxx\bar{y}$, the HYSCORE echo (including its nuclear amplitude modulation by nuclear coherence transfer echoes) and the crossing echo artifacts parallel to t_2 shift to the upper channel (Fig. 4b). After baseline correction, the time-domain signals in Fig. 4c are obtained. The upper channel is now free of artifacts. The echo crossings parallel to the $t_1 = t_2$ diagonal are clearly visible in the lower channel, as they are not removed by baseline correction.

Analogous to three-pulse ESEEM, the signal contamination from (0, 0, 0, −) has the same phase as the echo of interest and can only be removed by applying a 16-step cycle $x(x)(x)(y)$, if necessary.

6.4 Five-Pulse ESEEM

In the five-pulse ESEEM experiment [14], [90°–τ_1–180°–τ_1–90°–T–90°–τ_2–180°–τ_2–detect], the signal is acquired as a function of T. There are three focused pathways contributing to the signal: the unwanted two-pulse echo (0, 0, 0, +, −) (designated henceforth as E_0) and the two wanted five-pulse echoes (+, −, 0,

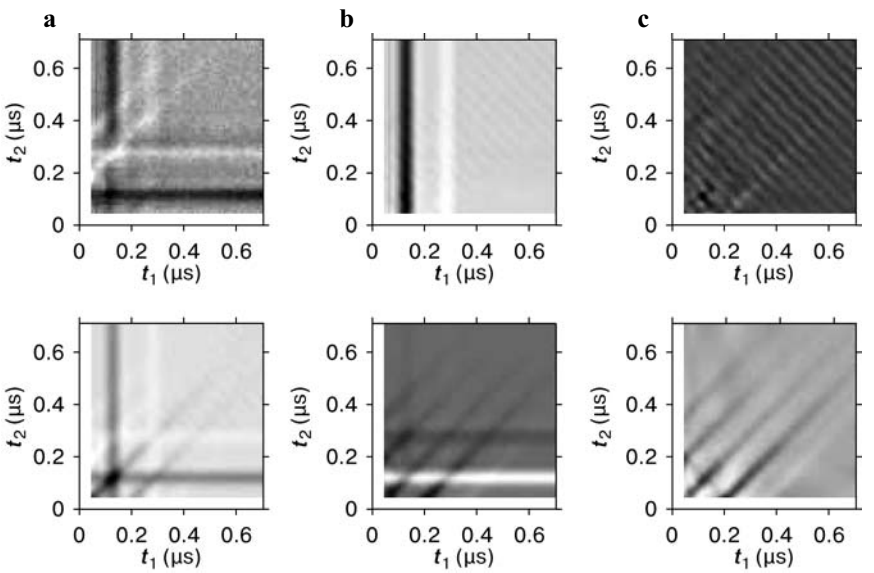

Fig. 4. HYSCORE time-domain signals from coal (9.6380 GHz, 343.44 mT, room temperature). **a** Pulse phases *xxxx*, **b** pulse phases $xxx\bar{y}$, **c** data from **b** after baseline correction along t_2 and t_1. Parameters: $\tau = 140$ ns, $t_{1,0} = t_{2,0} = 48$ ns, $\Delta t_1 = \Delta t_2 = 8$ ns. Top, channel A; bottom, channel B. The greyscales in the six plots are not to scale.

+, −) and (−, +, 0, +, −) (labelled as E_+ and E_-, respectively), whose amplitudes are modulated along T.

The signals of the two wanted pathways are given by $E_\pm = V_0 \pm V_{\mathrm{mod}}(T)$, where V_0 is the unmodulated part, and V_{mod} is the modulating one [17]. If all pulses have the same phase, the two pathway signals have the same phase, E_+ and E_- add, and the modulating parts of the two pathways cancel. If the third pulse is phase-shifted by 90°, the signals of the two pathways shift by 90° in opposite directions, since $\Delta p_3 = \pm 1$. As a consequence, they are now phase-shifted by 180°, so that E_+ and E_- are subtracted, and the modulating components add up, whereas the constant parts cancel. The conventional choice of phases to achieve this subtraction is *yyxxx* [14, 17]. In a full analysis it turns out that the only requirement to obtain the subtraction is that the first and the third pulse have to be orthogonal. The phases of the other pulses are irrelevant.

The two-step phase cycle *yyx*(*xx*) as given in ref. 14 removes all crossing echoes but retains the two-pulse echo from the focused pathway (0, 0, 0, +, −). This is usually of little concern, as it is phase-shifted by 90° with respect to the two pathway signals of interest. Its out-of-phase component, if present, only adds a possibly sloping baseline to the five-pulse ESEEM signal. For quantitative work it should be suppressed using a four-step cycle, e.g., *yy*(*x*)(*xx*). If the spectrometer has only available 180° phase shifts, phase-cycled five-pulse ESEEM cannot be implemented.

The fact that there are two fixed delay lengths, τ_1 and τ_2, complicates the analysis substantially. In the special cases $\tau_1 = \tau_2$, $\tau_1 = 2\tau_2$ and $2\tau_1 = \tau_2$, there exist additional focused three-pulse echoes that coincide with the two five-pulse echoes: (0, +, 0, 0, −), (+, 0, 0, 0, −) and (+, +, 0, −, −) for $\tau_1 = \tau_2$, (0, +, 0, −, −) and (+, 0, 0, −, −) for $\tau_1 = 2\tau_2$, and (+, +, 0, 0, −) for $2\tau_1 = \tau_2$. Even for small deviations from these conditions, the echoes form very close to the detection point, so that they may interfere. It is not clear whether their modulations are generally in phase with the modulations of the five-pulse echoes or not. However, due to the pulse flip angles employed, the amplitudes of these echoes are usually small and can be neglected. If not, the eight-step phase cycle *y*[*y*](*x*)*xx* removes them.

The four-step phase cycle from [17] cannot be written in our shorthand notation, as it is not a nested cycle. In explicit form, it consists of the steps *yyxxx*, $yyx\bar{x}\bar{x}$, $\bar{y}yxx\bar{x}$ and $\bar{y}yx\bar{x}x$ with the LC coefficients +1, −1, −1, +1, if we phase-invert the original steps 2 and 3 to remove the receiver offset. This cycle removes all crossing echoes but retains (0, 0, 0, 0, −). Interestingly, it eliminates (+, +, 0, 0, −) for $2\tau_1 = \tau_2$, in contrast to the four-step cycle *yy*(*x*)(*xx*).

6.5 Six-Pulse HYSCORE

The six-pulse HYSCORE experiment [15, 17], [90°–τ_1–180°–τ_1–90°–t_1–180°–t_2–90°–τ_2–180°–τ_2–detect], with pulse phases *yyxxxx*, is based on five-pulse ESEEM, where a 180° pulse dividing the delay T into t_1 and t_2 is inserted. The echo amplitude is measured as a two-dimensional function of t_1 and t_2. As in five-pulse

ESEEM, there are three focused pathways: the wanted (±, ∓, 0, 0, +, −), and the unwanted (0, 0, 0, 0, +, −). For the special cases $\tau_1 = \tau_2$, $\tau_1 = 2\tau_2$ and $2\tau_1 = \tau_2$, there are again additional focused but unwanted three-pulse echo pathways. However, these have very small amplitude and can usually be neglected.

The pulse phasing with the four-step cycle $xx(y)(\bar{x})yx$ proposed in ref. 15 is ineffective, as it actually eliminates the signals of interest and retains many crossing echoes. But it can be corrected if the first two pulses are cycled together with the third pulse, i.e., $(xxy)(\bar{x})yx$. Then the phase cycle works properly and removes all but the three focused pathway signals, which have the correct relative phases. The phase cycle $(yyx)(x)xx$ as proposed in ref. 17 achieves the same result, as does the equivalent $yyx(x)(xx)$, which we prefer because of its consistency with the five-pulse ESEEM phase cycle. To eliminate the two-pulse echo due to (0, 0, 0, 0, +, −), an eight-step cycle like $yy(x)(x)(xx)$ is necessary. To completely eliminate all disturbing pathways for all τ_1, τ_2 combinations, an excessively long phase cycle might be necessary. In practice, the ones shown here seem to be suffcient.

6.6 Remote Echo Detection

Often, echo modulations in two-pulse ESEEM decay very rapidly so that it is indispensable to measure them for very small τ values. In the other ESEEM experiments, short τ values are often necessary to control the τ-dependent suppression of peaks. However, τ values ($= t_N$) cannot be shorter than the spectrometer's dead time. To circumvent this limit, an additional pulse block [90°–T_{re}–90°–τ_{re}–180°–τ_{re}] is appended to a pulse sequence, with the first pulse at the point where the echo of interest occurs and out of phase with this echo (remote echo detection, [16]). The first pulse stores the magnetization as polarization, which is then measured by the two-pulse-echo sequence. τ of the original sequence can now be chosen as short as necessary, and only τ_{re} must be larger than the dead time. This remote echo detection increases the number of coherence transfer pathways by a factor of 27 and the number of wanted pathways by a factor of two. Usually, T_{re} is chosen to be much longer than T_{2e} so that all pathways with coherence order ± 1 during that delay decay. But this is not mandatory. On the contrary, often it is desirable to keep T_{re} relatively short in order not to lose signal due to longitudinal relaxation.

Remote-echo-detected two-pulse ESEEM [16] requires four phases and four steps to remove all pathways except the two wanted, (±, ∓, 0, +, −), using the cycle $x[x]xxx$. This cycle also removes the pathway (0, 0, 0, 0, −). The eight-step cycle $x[x]x(xx)$ proposed in ref. 16 for the case $T_{re} < T_{2e}$ is not necessary, as the four-step cycle works for any length of T_{re}. This experiment is more difficult on spectrometers with only 180° phase shifts. In that case, the phase cycle $x(x)x(x)x$ can be used, which however keeps the unwanted three-pulse echo (+, +, 0, −, −).

In remote-echo-detected three-pulse ESEEM, the focused pathways are (±, 0, ∓, 0, +, −) and (0, 0, 0, +, −). Only the first two are wanted. If one can tolerate the two-pulse echo and the transient from (0, 0, 0, 0, −), the two-step cycle $xx(xxxx)$ is sufficient. Among the many four-step phase cycles that yield

the wanted pathways only, $(x)(x)xxxx$ is a possible choice. In the special case $2\tau = \tau_{re}$, the additional pathway $(+, 0, +, 0, 0, -)$ is focused, and an eight-step cycle like $(x)(x)xxx(x)$ would be required to cleanly eliminate its contribution, hence this particular choice of τ_{re} should be avoided.

For remote-echo-detected HYSCORE, there are many eight-step phase cycles that remove all unwanted crossing echoes, retaining only the wanted $(\mp, 0, 0, \pm, 0, +, -)$, if we assume $\Delta t_{lim} \approx 0$. One among these phase cycles is $(x)(x)(x)xxxx$. If the two-pulse echo of the last two pulses and the FID from the last pulse are of no concern, then $xx(x)(xxxx)$ can be used.

The remote-echo-detected version of five-pulse ESEEM is very complex, as it contains three different fixed delay lengths and eight pulses. When specific values of τ_1, τ_2 and τ_{re} are chosen, a full computer-aided pathway analysis is feasible and an effective phase cycle can be found. However, for arbitrary values, this is not possible anymore, and here we can only look at the limiting case $\Delta t_{lim} = 0$. It requires an eight-step cycle, e.g., $(yy)(x)(xx)yyy$ to suppress all crossing echoes and keep only $(\pm, \mp, 0, +, -, 0, +, -)$ and $(\pm, \mp, 0, -, +, 0, +, -)$. The four-step cycle $(yy)(x)xxyyy$ preserves in addition the focused unwanted $(\pm, \mp, 0, 0, 0, 0, +, -)$, but they are out of phase.

Remote-echo detection in six-pulse HYSCORE is a nine-pulse sequence, and the pathway analysis is lengthy. There are a total of 6561 pathways, of which over 1000 are visible, depending on the relative lengths of τ_1, τ_2, τ_{re} and the starting values of t_1 and t_2. The four wanted pathways are $(\pm, \mp, 0, 0, +, -, 0, +, -)$ and $(\pm, \mp, 0, 0, -, +, 0, +, -)$. With the simplifying assumption $\Delta t_{lim} = 0$, the cycle $yyx(x)(xxyyy)$ keeps all focused echoes and the last-pulse FID. $(yy)(x)(x)xxyyy$ removes all crossing signals, and sends all focused unwanted ones out of phase. One of the many 16-step cycles that eliminate all unwanted signals in this limiting case is $(yy)(x)(x)(x)xyyy$.

7 Conclusions

We have used a general procedure to devise and evaluate phase cycles for ESEEM experiments. The method is based on first determining electron coherence transfer pathways that contribute to the measured signal and then finding a nested phase cycle that specifically blocks the unwanted ones while retaining the desired ones.

We have applied the method to several standard and advanced ESEEM sequences, with up to nine pulses. As a result, we obtained several recommendable phase cycles for each experiment. Most known and published phase cycles are found valid. We have proposed new phase cycles for several experiments including remote echo detection.

We have found unconventional pulse phasings for three-pulse ESEEM (xxy) and HYSCORE ($xxxy$) which render phase cycling superfluous in the case of a symmetrically excited line. As this is of course a special case, and as there exist short phase cycles for these experiments, these phasings are in practice irrelevant for simple sequences. However, the underlying concept of reducing the number of necessary steps in a phase cycle by shifting the phase of the last pulse is

interesting and can be useful as a work-around for long pulse sequences where proper phase cycling would require too many steps.

For experiments with more than six pulses, the compact phase cycles given in this work are not guaranteed to be effective for all combinations of fixed delay lengths that appear in the sequence. If they are found to be incomplete, it is best to use the presented method to devise a phase cycle tailored to the particular combination of delay lengths at hand.

All phase programs in this paper are nested phase cycles. It might be possible that a more complete search will discover more effective phase programs with fewer steps in some cases.

Acknowledgments

We thank Gunnar Jeschke and Troy A. Stich for valuable comments on the manuscript. This work was supported by the Swiss National Science Foundation.

References

1. Bodenhausen, G., Kogler, H., Ernst, R.R.: J. Magn. Reson. **58**, 370–388 (1984)
2. Gemperle, C., Aebli, G., Schweiger, A., Ernst, R.R.: J. Magn. Reson. **88**, 241–256 (1990)
3. Levitt, M.H.: Spin Dynamics: Basics of Nuclear Magnetic Resonance, pp. 600–626. Wiley, Chichester (2001)
4. Jerschow, A., Müller, N.: J. Magn. Reson. **134**, 17–29 (1998)
5. Ollerenshaw, J., McClung, R.E.D.: J. Magn. Reson. **143**, 255–265 (2000)
6. Levitt, M.H., Madhu, P.K., Hughes, C.E.: J. Magn. Reson. **155**, 300–306 (2002)
7. Jerschow, A., Kumar, R.: J. Magn. Reson. **160**, 59–64 (2003)
8. Grandinetti, P.J.: Solid State Nucl. Magn. Reson. **23**, 1–13 (2003)
9. Ivchenko, N., Hughes, C.E., Levitt, M.H.: J. Magn. Reson. **160**, 52–58 (2003)
10. Hughes, C.E., Carravetta, M., Levitt, M.H.: J. Magn. Reson. **167**, 259–265 (2004)
11. Zuckerstätter, G., Müller, N.: J. Magn. Reson. **181**, 244–253 (2006)
12. Zuckerstätter, G., Müller, N.: Concepts Magn. Reson. **30**A, 81–99 (2007)
13. Fauth, J.-M., Schweiger, A., Braunschweiler, L., Forrer, J., Ernst, R.R.: J. Magn. Reson. **66**, 74–85 (1986)
14. Gemperle, C., Schweiger, A., Ernst, R.R.: Chem. Phys. Lett. **178**, 565–571 (1991)
15. Song, R., Zhong, Y.C., Noble, C.J., Pilbrow, J.R., Hutton, D.R.: Chem. Phys. Lett. **237**, 86–90 (1995)
16. Cho, H., Pfenninger, S., Gemperle, C., Schweiger, A., Ernst, R.R.: Chem. Phys. Lett. **160**, 391–395 (1989)
17. Kasumaj, B., Stoll, S.: J. Magn. Reson. **190**, 233–247 (2008)
18. Van Doorslaer, S., Schweiger, A.: Chem. Phys. Lett. **281**, 297–305 (1997)
19 Schweiger, A., Jeschke, G.: Principles of Pulse Electron Paramagnetic Resonance. Oxford University Press, Oxford (2001)
20. Szosenfogel, R., Goldfarb, D.: Mol. Phys. **95**, 1295–1308 (1998)
21. Mádi, Z.L., Van Doorslaer, S., Schweiger, A.: J. Magn. Reson. **154**, 181–191 (2002)
22. Stoll, S., Schweiger, A.: J. Magn. Reson. **163**, 248–256 (2003)
23. Levitt, M.H.: J. Magn. Reson. **126**, 164–182 (1997)
24. Reichert, D., Hempel, G.: Concepts Magn. Reson. **14**, 130–139 (2002)

Authors' address: Stefan Stoll, Department of Chemistry, University of California, Davis, One Shields Avenue, Davis, CA 95616, USA
E-mail: sstoll@ucdavis.edu